ACADEMIC PRESS

Available online at www.sciencedirect.com

SCIENCE DIRECT®

VIROLOGY

Virology 312 (2003) 350–358

www.elsevier.com/locate/yviro

Targeted cleavage of hepatitis E virus 3′ end RNA mediated by hammerhead ribozymes inhibits viral RNA replication

Bandi Sriram, Deepshi Thakral, and Subrat Kumar Panda*

Department of Pathology, All India Institute of Medical Sciences, Ansari Nagar, New Delhi 110029, India

Received 13 November 2002; returned to author for revision 13 February 2003; accepted 3 March 2003

Abstract

The 3′ end of hepatitis E virus (HEV) contains *cis*-acting regulatory element, which plays an important role in viral replication. To develop specific replication inhibitor at the molecular level, mono- and di-hammerhead ribozymes (Rz) were designed and synthesized against the conserved 3′ end sequences of HEV, which cleave at nucleotide positions 7125 and 7112/7125, respectively. Di-hammerhead ribozyme with two catalytic motifs in tandem was designed to cleave simultaneously at two sites spaced 13 nucleotides apart, which increases the overall cleavage efficiency and prevents the development of escape mutants. Specific cleavage products were obtained with both the ribozymes in vitro at physiological conditions. The inactive control ribozymes showed no cleavage. The ribozymes showed specific inhibition of HEV 3′ end fused-luciferase reporter gene expression by ~37 and ~60%, respectively in HepG2 cells. These results demonstrate a feasible approach to inhibit the HEV replication to a limited extent by targeting the *cis*-acting 3′ end of HEV with hammerhead ribozymes.

Keywords: *Trans*-acting; *Cis*-acting; Gene expression; Gene therapy; Transient expression

Introduction

Hepatitis E virus (HEV) is the major causative agent for feco-orally transmitted epidemic and sporadic acute viral hepatitis in many developing countries (Purcell and Ticehurst, 1988; Bradely, 1990). The HEV genome is a positive-sense, capped, and polyadenylated RNA of around 7.2 kb in length, containing three open reading frames (ORFs) (Purdy et al., 1993; Panda and Jameel, 1997; Kabrane et al., 1999; Tyagi et al., 2002). The coding sequence in the HEV genome is flanked by 5′ and 3′ noncoding regions (NCRs) that are 27 and 68 nucleotides long (Kabrane et al., 1999). It has been demonstrated that the 3′ noncoding region of HEV forms stem–loop structures that contain *cis*-acting elements which interact with viral RNA-dependent RNA polymerase (RdRp) and cellular proteins required for virus replication (Song and Simon, 1995; Agrawal et al., 2001). The inhibition of this interaction can block the viral replication. We attempted to achieve the same by using designed ribozymes. Ribozymes are RNA molecules that catalyze cleavage of a target RNA molecule based on sequence-specific recognition (Uhlenbeck, 1987) and may have potential therapeutic applications (James and Shamhkani, 1995). Ribozymes have been previously used to inhibit gene expression in viruses like HIV, HBV, and HCV and also neoplastic cells (Dahm and Uhlenbeck, 1991; Chen et al., 1992; Parthasarathy et al., 1999; Macejak et al., 2000). This report demonstrates in vitro and intracellular cleavage of HEV RNA covering the RdRp binding domain by designed ribozymes.

Results

In vitro cleavage of HEV 3′ end RNA by ribozymes

The hammerhead ribozymes were designed to cleave HEV 3′ end RNA in the stem–loop 2 region. Two target sites, GUA and GUU at nucleotide (nt) positions 7112 and 7125, were selected from published secondary structure of

* Corresponding author. Fax: +91-11-26588663.
E-mail address: pandask@hotmail.com (S.K. Panda).

0042-6822/03/$ – see front matter © 2003 Elsevier Science (USA). All rights reserved.
doi:10.1016/S0042-6822(03)00259-9

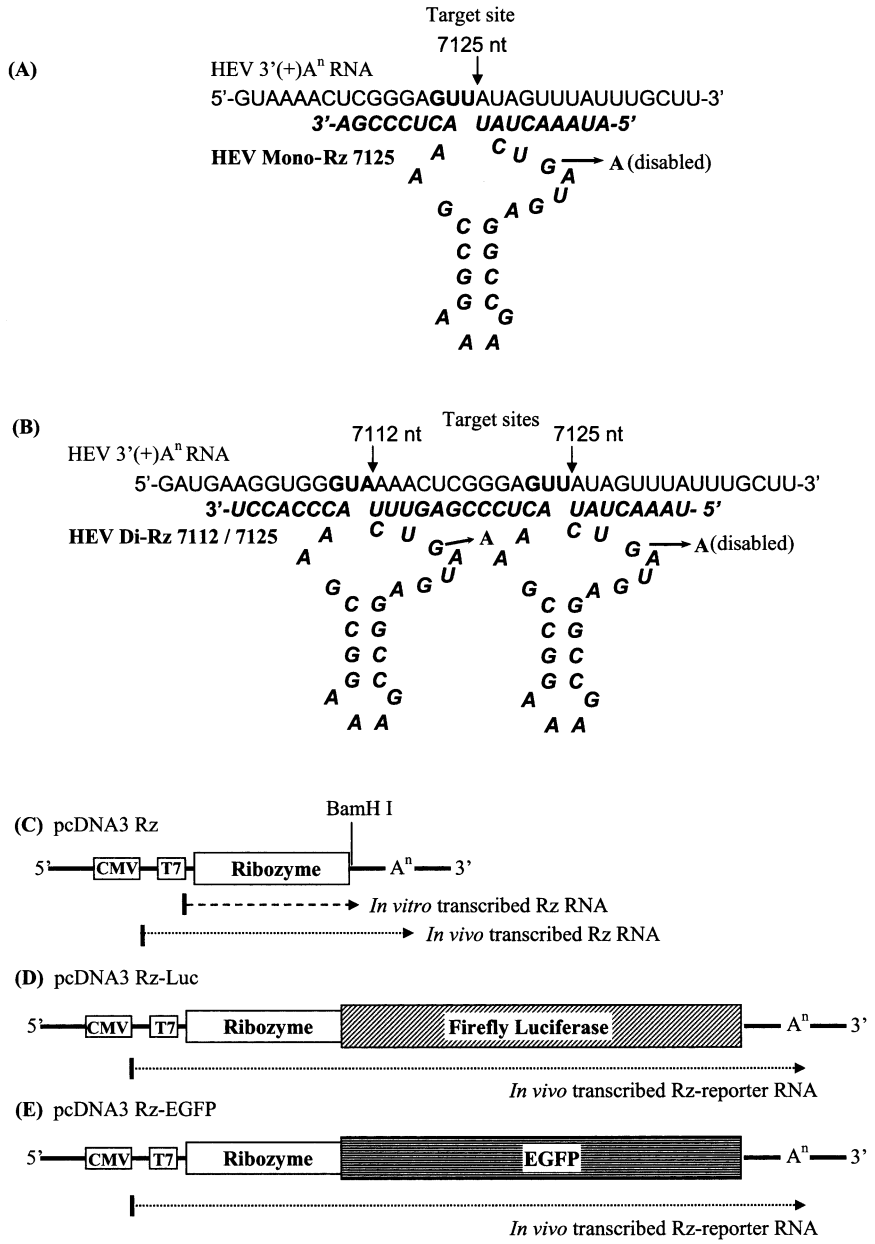

Fig. 1. Design of ribozymes and structures of ribozyme expression vectors. (A) Specific hybridization of Mono-Rz 7125 with target RNA at site GUU (7125). Cleavage after U is indicated by arrow. (B) Specific hybridization of Di-Rz 7112/7125 with target RNA at target sites GUA (7112) and GUU (7125). Cleavages after A and U are indicated by arrows. Inactive control Rz with point mutation in catalytic motif G5→A is also shown. (C) Structure of ribozyme expression vector, showing in vitro transcribed Rz RNA from T7 promoter and in vivo transcribed Rz RNA from CMV promoter by dashed arrows. (D) Structure of ribozyme-fused firefly luciferase reporter vector. (E) Structure of ribozyme-fused EGFP reporter vector.

HEV 3′ end RNA (Agrawal et al., 2001). Mono-hammerhead ribozyme was designed against the target site GUU (7125), as shown in Fig. 1A. A Di-hammerhead ribozyme was designed against two target sites GUA (7112) and GUU (7125), as shown in Fig. 1B. The sense and antisense ribozyme oligonucleotides were synthesized, annealed, and cloned in the plasmid vector pcDNA3 (Invitrogen, The Netherlands). Two ribozyme controls, one that is catalytically inactive due to a point mutation G5 to A in the catalytic motif and the other with scrambled binding arms, were also synthesized and cloned. Sequences of all the ribozyme clones were confirmed.

Activities of the designed ribozymes were tested in vitro, using target RNA and ribozyme RNA transcribed by T7 RNA polymerase from their respective plasmid vectors after linearization at the 3′ end of the construct. The transcript sizes were 77 nt for the Di-Rz 7112/7125 and 44 nt for the Mono-Rz 7125, respectively (Fig. 3A, lanes 1 and 5). The transcript size of HEV 3′ end target RNA was 115 nt (Fig. 3A, lane 3), which was obtained from the plasmid pUC18-

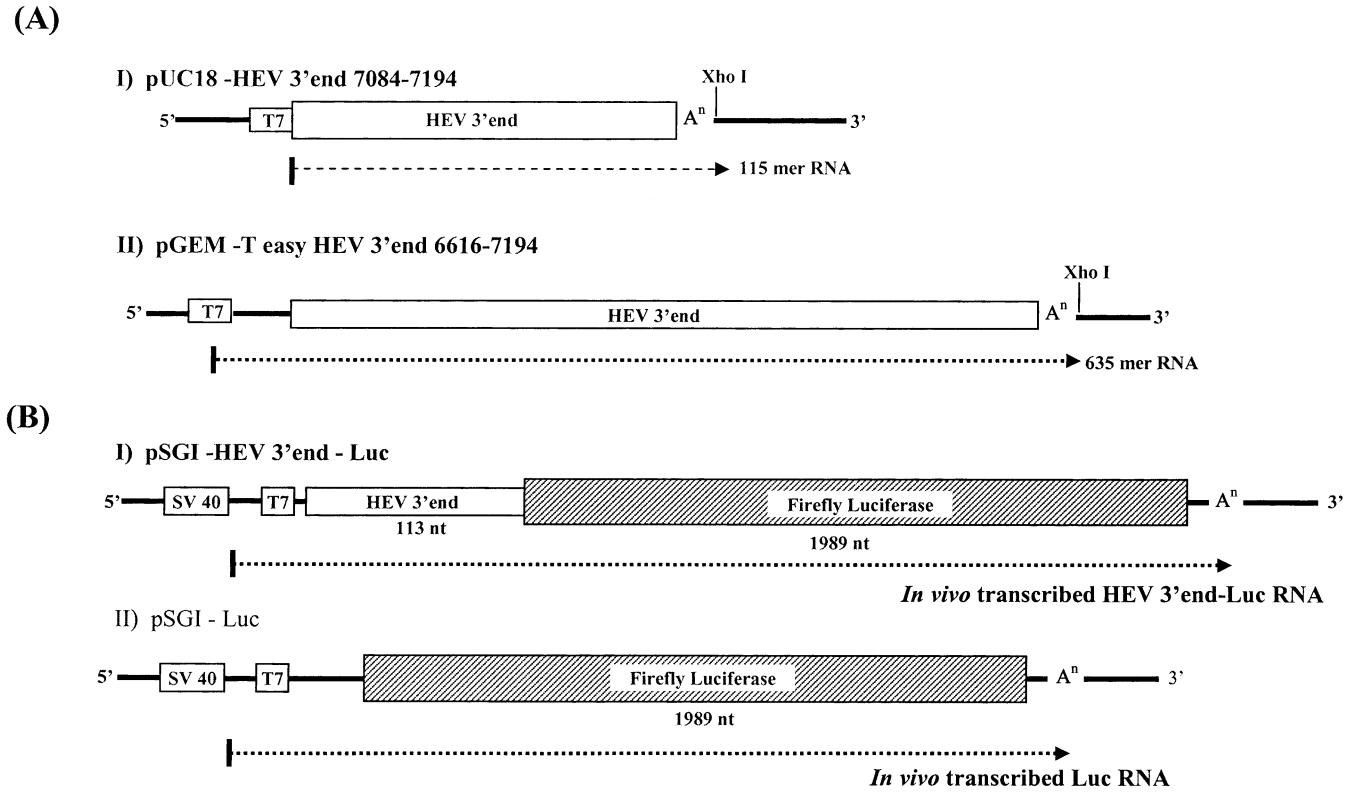

Fig. 2. Structures of HEV 3′ end and HEV 3′ end-fused Luciferase containing vectors. (A) Structure of HEV 3′ end vectors used for in vitro assays showing template RNA transcripts made from T7 promoter of lengths 115 nt (I) and 635 nt (II) by dashed arrows. (B) Structure of HEV 3′ end fused Luciferase vector pSGI-HEV 3′ end-Luc (I) and vector pSGI-Luc lacking HEV 3′ end (II) used for in vivo assays. SV40 early promoter initiated intracellular expression from these vectors.

HEV 3′ end 7084–7194 (Fig. 2A and I). The cleavage reactions were carried out with the [α-^{33}P]UTP-labeled HEV 3′ end RNA and unlabeled Rz (heat denatured) in equimolar amounts (0.27 pmol each) under the standard cleavage conditions (50 mM Tris–HCl, pH 7.5, 10 mM $MgCl_2$) and incubated at 37°C for 2 h. Di-Rz 7112/7125 cleaved the HEV 3′ end substrate RNA into 74, 41, 28, and 13 nt fragments (Fig. 3A, lane 2), whereas Mono-Rz 7125 cleaved the substrate RNA into 74- and 41-nt fragments (Fig. 3A, lane 4). The control-disabled ribozymes showed no cleavage (Fig. 3C, lanes 1–4), indicating that the cleaved products obtained were due to active ribozymes. The Di-Rz 7112/7125 and Mono-Rz 7125 cleaved up to 90 and 40% of the target RNA. The cleavage efficiency of both the ribozymes were tested at physiologically relevant concentrations of $MgCl_2$ (1–2 mM) and significant cleavages were achieved by Di-Rz ~38% (Fig. 3D, lanes 3 and 4) and by Mono-Rz ~10% (Fig. 3E, lanes 3 and 4). No cleavage was observed in the absence of $MgCl_2$ (Fig. 3D and E, lane 2). Both the ribozymes cleave HEV 3′ end RNA in a sequence-specific manner that is protein-independent (Dahm and Uhlenbeck, 1991; Santoro and Joyce, 1997). The bands were quantified using a Bio-Rad GS-525 molecular imager (Bio-Rad Laboratories, USA). Using similar experimental conditions, cleavage efficiency of both the ribozymes were tested against longer HEV 3′ end transcript of 635 nt in length transcribed from the plasmid pGEM-T Easy HEV 3′ end 6616-7194 (Fig. 2A, II and Fig. 3B, lane 1). The cleaved products were observed as expected (Fig. 3B, lanes 2–5) and cleavage was also obtained without heat denaturation (90°C, 2 min) of the transcript (Fig. 3B, lanes 4 and 5), indicating that both the ribozymes could access the target site even when the native secondary folding of the RNA is maintained. The cleavage rate was determined by taking varying amounts of labeled HEV 3′ end substrate RNA under ribozyme saturating conditions. The K_m and the K_{cat} for the Di-Rz were 2.5×10^{-13} M and 4.76×10^{-5} min^{-1}, respectively, and for the Mono-Rz 5.5×10^{-13} M and 1.2×10^{-5} min^{-1}, respectively. The kinetic parameters suggest that the Di-Rz 7112/7125 was more efficient of the two.

Intracellular expression of ribozymes

To determine the intracellular expression of ribozymes, slot-blot hybridization analysis of the total cellular RNA from cells transfected with the ribozyme expression vector pcDNA3 Rz was used (Fig. 1C). Radiodensitometry analysis showed that active and inactive ribozyme RNA were expressed at about equal levels from transfected cells (Fig. 4A). Total cellular RNA was hybridized with radiolabeled antisense Di-Rz probe in slots 2a (Di-Rz) and 2b (Di-Rz mut) and antisense Mono-Rz probe in slots 2c (Mono-Rz)

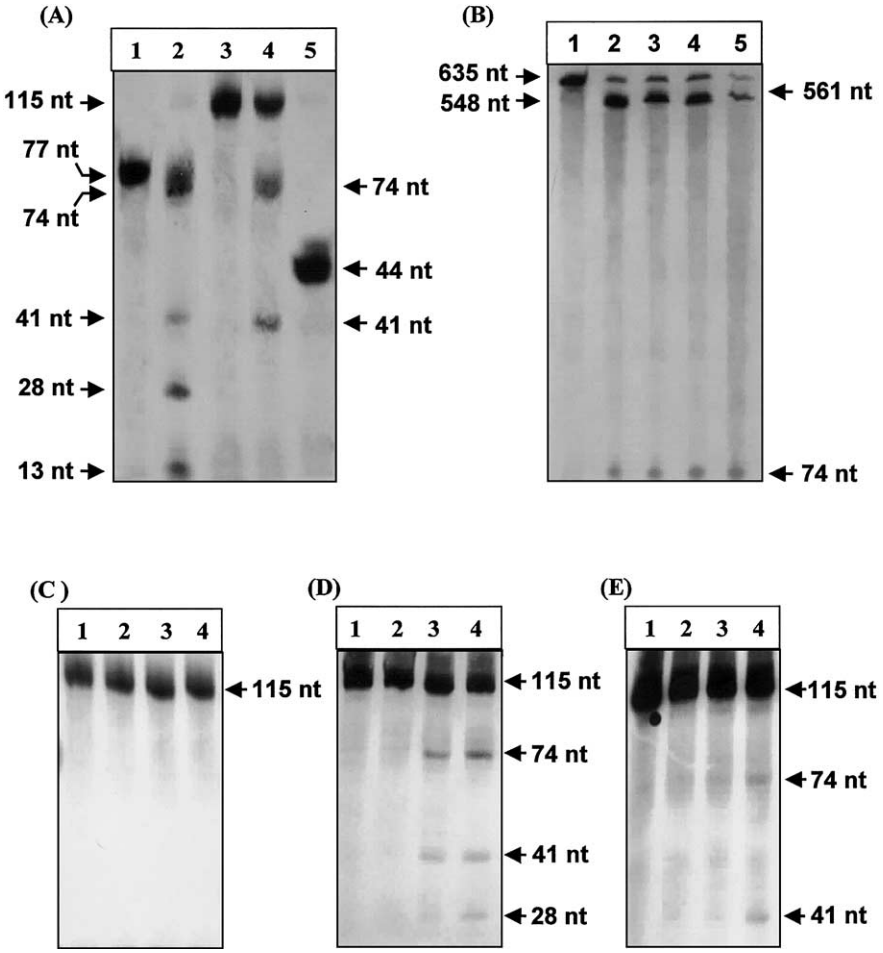

Fig. 3. In vitro cleavage analyses of HEV 3′ end RNA by ribozymes. (A) Cleavage of HEV 3′ end RNA of length 115 nt, lane 1 and 5 shows sizes of Di-Rz 7112/7125 (77 nt) and Mono-Rz 7125 (44 nt). Uncleaved HEV 3′ end RNA transcript of length 115 nt is shown in lane 3. Cleavage of HEV 3′ end RNA into cleaved products 74, 41, 28, and 13 nts by Di-Rz 7112/7125 (lane 2) and by Mono-Rz 7125 into cleaved products 74 and 41 nts (lane 4). (B) Cleavage of HEV 3′ end longer transcript of length 635 nt. Lane 1 shows uncleaved target RNA. Lane 2 and 3 shows cleavage by Di-Rz 7112/7125 and Mono-Rz 7125 along with cleaved products. Efficient cleavage of target RNA by Di-Rz 7112/7125 (lane 4) and Mono-Rz 7125 (lane 5) was also observed without heat denaturation step (90°C for 2 min.). (C) Cleavage with catalytically inactive ribozymes. (Lane 1) Di-Rz (mut), (lane 2) Di-Rz (dis), (lane 3) Mono-Rz (mut), and (lane 4) Mono-Rz (dis). All the lanes show no cleaved products of the target RNA. (D) and (E) Cleavage at physiological $MgCl_2$ concentration. Lanes 3 and 4 of (D) and (E) show cleavage at 1 and 2 mM of $MgCl_2$ of Di-Rz and Mono-Rz respectively. No cleavage without $MgCl_2$ in lane 2 and lane 1 shows only substrate transcript of length 115 nt.

and 2d (Mono-Rz mut) to detect the sense Rz RNA. Slots 1a, 1b, 1c, and 1d show that none of the probes hybridize with RNA from untransfected control cells (Feng et al., 2001). The intracellular expression of ribozymes was further confirmed by ribozyme-fused reporter gene vectors pcDNA3 Rz-Luc (firefly luciferase) (Fig. 1D) and pcDNA3 Rz-EGFP (enhanced green fluorescent protein) (Fig. 1E) in transient transfection assay in HepG2 cells. Reporter gene expression levels were found to increase with increasing concentrations of the vector DNA (Fig. 4B and C).

Intracellular cleavage of HEV 3′ end RNA by ribozymes

The activity of endogenously expressed ribozymes were tested in HepG2 cells by use of a target–reporter vector pSGI-HEV 3′ end–Luc generated by fusing HEV 3′ end and firefly luciferase (Luc) gene under the control of SV40 early promoter (Fig. 2B, I). The effects of the ribozymes were analyzed by cotransfection experiments using equal concentrations (1 μg each) of the ribozyme and reporter target vector followed by luciferase assay. Plasmid pRL-SV40 (Promega, USA) carrying Renilla luciferase (R-Luc) gene served as an internal control. The reduction of luciferase activity by ~60% (Di-Rz 7112/7125) and ~37% (Mono-Rz 7125) respectively (Fig. 5A) was observed. The catalytically inactive ribozymes (Rz mut) also down-regulated the luciferase expression in this system. However, the extent of this inhibition (~37% by Di-Rz 7112/7125 mut and ~22% by Mono-Rz 7125 mut, Fig. 5A) was much less than that produced by the active ribozymes. This inhibitory effect was likely to be from an antisense effect that destabilises the mRNA by base pairing. This was further substantiated by

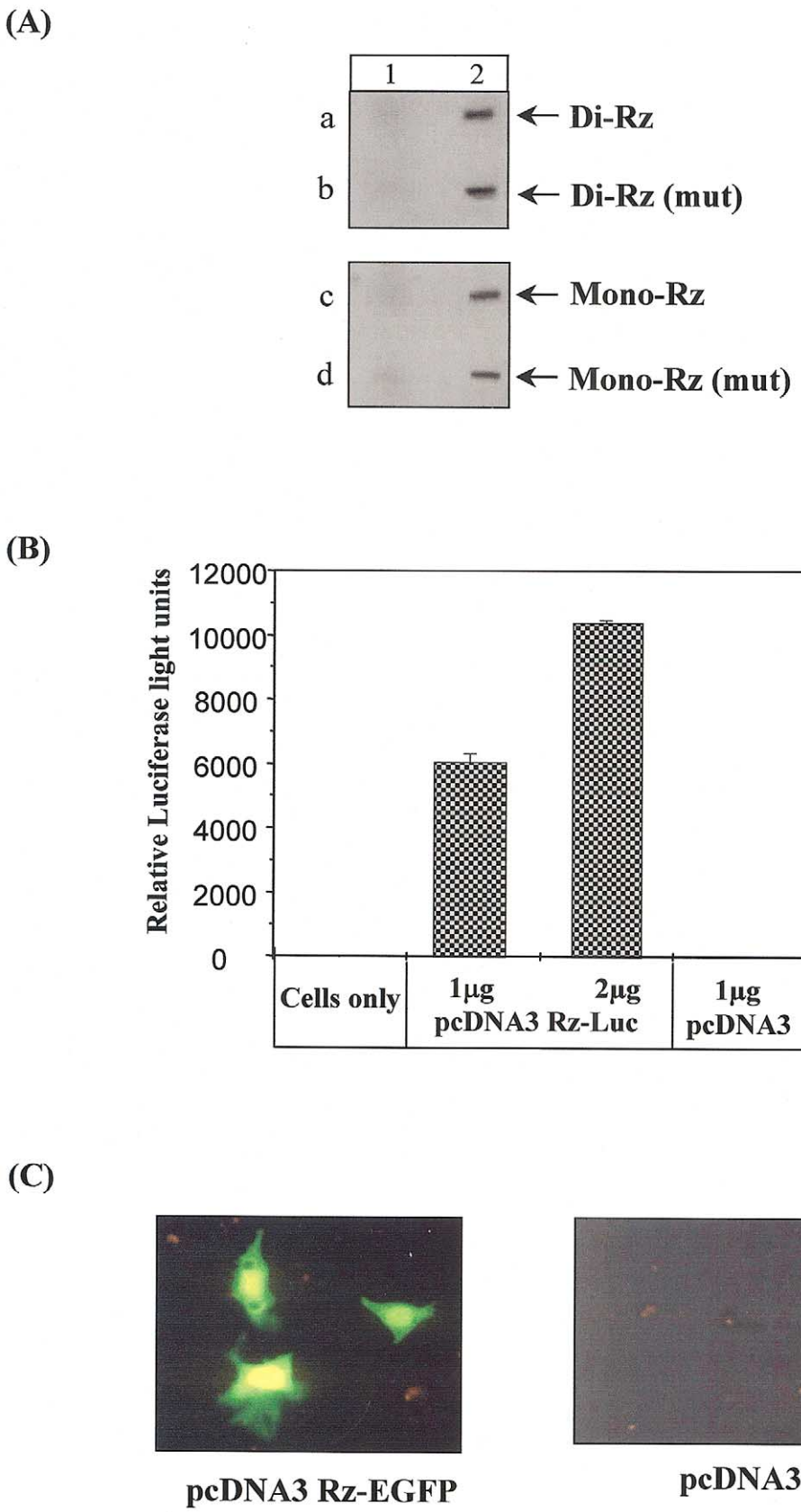

Fig. 4. Intracelluar expression of anti-HEV ribozymes. (A) Ribozyme expression of plasmids pcDNA3 Di-Rz/Mono-Rz in transfected HepG2 cells was verified by using slot-blot analysis of total cellular RNA. Thirty micrograms of total cellular RNA were hybridized with radiolabeled ribozyme antisense probe Di-Rz in lanes 2a (Di-Rz) and 2b (Di-Rz mut) and antisense Mono-Rz probe in lanes 2c (Mono-Rz) and 2d (Mono-Rz mut). Lanes 1a, 1b, 1c, and 1d show no hybridization since the RNA blotted was from untransfected cells. (B) One and 2 μg of ribozyme-fused firefly luciferase reporter vector pcDNA3 Rz-Luc were transfected and assayed for luciferase assay. Luciferase expression levels were found to increase with increase in dose. (C) Two micrograms of ribozyme-fused EGFP reporter vector pcDNA3 Rz-Luc were transfected and the green fluorescence was observed by confocal microscopy. Cells only and parent vector pcDNA3 show no expression levels.

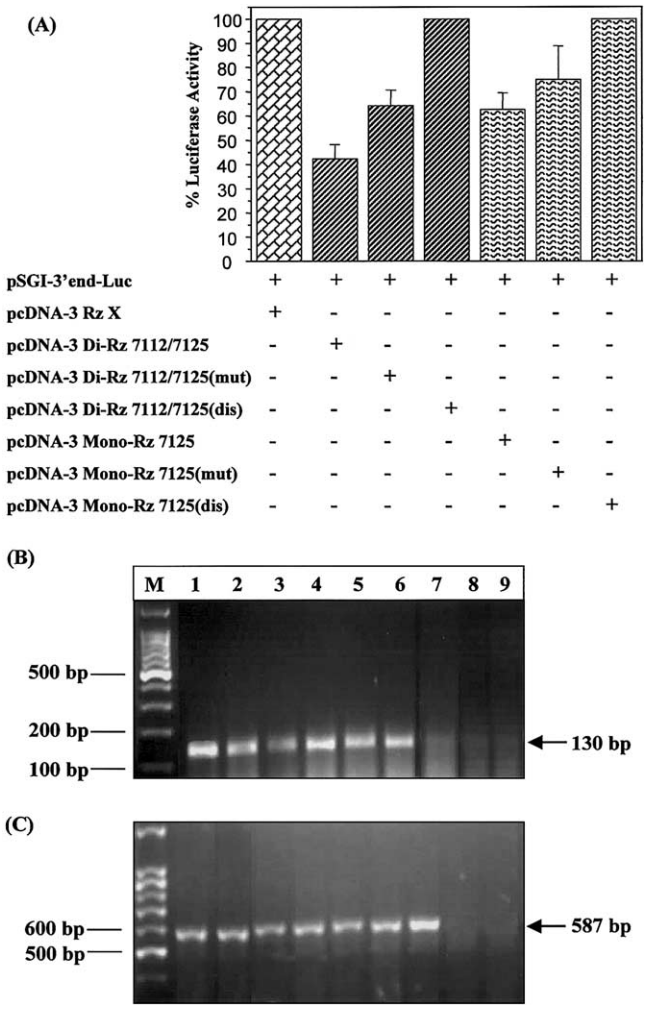

Fig. 5. Intracellular cleavage of HEV 3′ end RNA by ribozymes. (A) Cotransfection of pcDNA3 Rz and pSGI-HEV 3′ end-Luc plasmids. Both Mono-Rz and Di-Rz interfered very efficiently in luciferase expression. Inhibition of luciferase expression was also found in the case of mutant ribozymes (Rz mut). Disabled ribozymes (Rz dis) at equivalent concentrations had no effect on the levels of luciferase activity. The extent of luciferase activity detected by cotransfecting 1 μg of pSGI-HEV 3′ end-Luc and 1 μg of unrelated pcDNA3 Rz X was taken as 100%. Renilla luciferase activity was detected to normalize the variation of transfection efficiency among different samples. Shown are the mean ± SD from three separate experiments. (B) Reduction in HEV 3′ end RNA by ribozymes detected by RT–PCR. (Lane 1) The amount of HEV 3′ end RNA detected from cells transfected only with pSGI-HEV [I] plasmid (1 μg). When cotransfected with 3 μg of each Mono-Rz (lane 2) and Di-Rz (lane 3) plasmids, reduced expression was found that was quantitated by real-time PCR from the standard curve plotted using SYBR-Green PCR master mix. Rz X, disabled Mono-, and Di-Rzs (lanes 4, 5, and 6) showed no reduction in the levels of target RNA. RT–PCR controls in lane 7 (cells only), lane 8 (without reverse transcriptase enzyme), and lane 9 (without template) showed no amplification. (C) The same amounts of lysates were used as in B and levels of the control RNA was determined for the hGAPDH gene using its specific terminal primers. The levels of control RNA in all corresponding lysates remained unchanged.

the observation that the disabled ribozymes (Rz dis) with scrambled binding arms showed no inhibition in the luciferase expression. pcDNA3 Rz X, a nonspecific ribozyme directed against HIV-1 *gag* sequence, also failed to inhibit luciferase expression (Fig. 5A).

Using infectious HEV clone pSGI-HEV [I] (Panda et al., 2000), reduction in the HEV 3′ end RNA by ribozymes was detected by reverse transcription–polymerase chain reaction (RT–PCR) and quantified by real-time PCR using the SYBR-Green dye method. Lane 1 in Fig. 5B shows the levels of HEV 3′ end RNA when 1 μg of pSGI-HEV [I] plasmid alone was transiently expressed. Lanes 2 and 3 show the levels of RNA when cotransfected with 3 μg of pcDNA3 Mono-Rz and pcDNA3 Di-Rz, and lanes 4, 5, and 6 show those when cotransfected with 3 μg of each Rz X, disabled Di-Rz, and disabled Mono-Rz, respectively. The RT–PCR controls, lane 7 (plain cells), lane 8 (without reverse transcriptase enzyme), and lane 9 (without template) showed no amplification. The human glyceraldehyde-3-phosphate dehydrogenase (hGAPDH) was also amplified from the equivalent amount of cell lysate that served as an internal control (Weinberg et al., 2000). The hGAPDH RNA levels observed after RT–PCR remained the same in all corresponding lanes (Fig. 5C). Real-time RT-PCR assay was used to measure quantitatively total levels of HEV 3′ end RNA from the standard curve of HEV 3′ end RNA using SYBR-Green PCR mix (Yang et al., 2002). The quantity of 3′ end HEV RNA was reduced by 30% (2.2×10^8 copies of RNA) by Mono-Rz and around 50% (1.6×10^8 copies of RNA) by Di-Rz in comparison to the levels in the cells transfected with pSGI-HEV [I] plasmid alone (3.4×10^8 copies of RNA). From these observations it was deduced that the reduction was due to specific intracellular cleavage by ribozymes in these experiments.

Discussion

This study was designed to determine the use of hammerhead ribozymes to specifically target HEV RNA at the site of interaction with RdRp and to evaluate the efficacy of these *trans*-acting Mono- and Di-ribozymes in cleavage of HEV RNA in vitro and in HepG2 cells. Two target sites GUA (7112) and GUU (7125) were selected (Fig. 1A and B) on the basis of the confirmed secondary structure in the single-stranded region of the HEV 3′ end (Agrawal et al., 2001). The advantage of Di-Rz or multi-target Rzs is to increase the overall cleavage efficiency and to prevent the development of escape mutants. Multi-target ribozymes have been designed earlier by linking Mono-Rz against HIV and were found to be more efficient than Mono-Rzs (Chen et al., 1992). However, in those instances the target sites were distantly apart. In this study, we report a Di-Rz against two closely spaced target sites with an internal binding arm along with 5′ and 3′ terminal binding arms (Fig. 1B) and found that there was cleavage induced by the two motifs simultaneously (Fig. 3A, lane 2). Di-Rz was found more efficient in cleaving the substrate RNA under standard in vitro conditions than Mono-Rz 7125. This could be due to

the ability of Di-Rz to cleave substrate into multiple RNA fragments and increased turnover of the cleavage reaction as previously reported (Chen et al., 1992). We also found that both the ribozymes were equally efficient in cleaving the longer HEV transcript of 635 nt under standard in vitro cleavage conditions (Fig. 3B), which confirms the accessibility of the ribozymes to the target sites and sequence specificity of the cleavage. The important feature of both Rzs was their ability to cleave the target RNA at $MgCl_2$ concentrations of 1 and 2 mM (Fig. 3D and E, lanes 3 and 4), which are close to the physiological levels (Santoro and Joyce, 1997). The kinetic parameters of both the Rzs were found to be equally efficient when compared with the other Rzs and DNA enzymes that have been reported (Santoro and Joyce, 1997). This high efficiency could be due to the fact that the Rz RNA had no substantial proportions of vector sequences that could affect secondary structure of ribozymes, substrate binding, and cleavage steps.

Slot-blot hybridization and ribozyme-fused reporter gene assays confirmed the endogenous expression of anti-HEV ribozymes (Fig. 4A–C). Since there is no cell culture system available for HEV to evaluate the efficacy of these anti-HEV Rzs, target–reporter vector pSGI-HEV 3′ end–Luc (Fig. 2B) was used to demonstrate intracellular cleavage of HEV 3′ end RNA. Any cleavage in HEV 3′ end RNA would result in down-regulation of luciferase expression. Similar constructs have been used to evaluate Rzs and DNA enzymes against hepatitis C virus (HCV) (Sakamoto et al., 1996) and hepatitis B virus (HBV) (Macejak et al., 2000). Around 60% and 37% of inhibition in luciferase expression were found when Di-Rz and Mono-Rz plasmids were co-transfected with vector containing HEV 3′ end–Luc (Fig. 5A). This reduction in luciferase expression by anti-HEV ribozymes was comparable with other ribozymes (Sakamoto et al., 1996; Macejak et al., 2000). It is evident that whatever reduction in luciferase expression was observed was due to intracellular cleavage of HEV 3′ end RNA by active ribozymes (Sakamoto et al., 1996). We also observed reduction in luciferase expression levels by catalytically inactive point mutated ribozymes (Di-Rz 7112/7125 mut ~37%; Mono-Rz 7125 mut ~22%) (Fig. 5A). These mutant Rzs do not cleave its target RNA but still reduces gene expression, presumably due to an antisense effect. The higher inhibition by active ribozymes indicates that the active catalytic domain of the hammerhead ribozyme could increase the extent of inhibition on top of the antisense inhibition (Feng et al., 2001). This is not unexpected since the formation of helices I and III (Fig. 1A and B) is a prerequisite for mediating hydrolytic cleavage and potentially gives rise to an antisense effect (Feng et al., 2001). However, there are reports that the inhibition was more pronounced with the active ribozyme than with catalytically inactive one when applied exogenously (Bramlage et al., 1999). There was no reduction in luciferase expression by disabled Rzs with scrambled arms and with unrelated Rz X (Fig. 5A), which lacks the ability to hybridize to the substrate RNA. Therefore, the suppression of luciferase activity in the present study suggests that anti-HEV Rzs could access the target sites and cleave HEV 3′ end RNA intracellularly. The reduction in the HEV 3′ end RNA levels was demonstrated by RT–PCR and quantitative real-time PCR from cotransfection experiments of anti-HEV Rzs with the infectious HEV clone pSGI-HEV [I]. The reduction in the HEV 3′ end RNA levels by Mono-Rz (~30%) and Di-Rz (~50%) (Fig. 5B, lanes 2 and 3) were compared with the levels of the RT–PCR product of the HEV 3′ end (Fig. 5B, lane 1). As expected, unrelated Rz X and disabled ribozymes did not show any reduction in the target RNA levels (Fig. 5B, lanes 4–6). The corresponding lysates showed almost no reduction in the levels of the housekeeping RNA (hGAPDH) used as an internal control (Fig. 5C). Thus we conclude that anti-HEV Rzs cleave specifically HEV 3′ end RNA, which is generated from infectious HEV clone pSGI-HEV [I] in the transfected cells.

In summary, this report describes the efficacy of Mono- and Di-Rzs designed to cleave target HEV RNA both in vitro and in HepG2 cells. The potential therapeutic implication of such ribozymes in self-limiting infection to prevent development of liver failure needs to be investigated.

Materials and methods

Construction of ribozyme expression vector

Both sense and the complementary oligonucleotide sequences encoding ribozymes were synthesized on an automated DNA synthesizer (Model 392, Applied Biosystems, USA). Cleavage-deficient ribozymes, one with a G5 → A point mutation (Rz mut) in the catalytic domain of the hammerhead ribozyme (Fig. 1A and B), which allows binding to the target RNA but lacks the cleavage ability, and another with scrambled flanking sequences in the binding arms, which totally lacks binding capability to the target RNA (Rz dis), were also synthesized for control experiments. As an additional negative control, a known ribozyme (pcDNA3 Rz X), which was directed against *gag* region of HIV genome, was used for checking specificity of the designed anti-HEV ribozymes (this plasmid was a gift from Dr. Akhil C Banerjea, National Institute of Immunology, New Delhi, India). The oligonucleotides with 5′ *Hin*dIII and 3′ *Bam*HI cohesive ends (added during synthesis) were phosphorylated, annealed, and cloned into the equivalent restriction sites of the vector pcDNA3 (Invitrogen, The Netherlands). The plasmids were named as pcDNA3 Rz 7125 and pcDNA3 Rz 7112/7125.

Construction of ribozyme-fused reporter gene vectors

Reporter genes, firefly luciferase (Luc) and enhanced green fluorescent protein (EGFP), were fused with anti-HEV ribozyme gene individually to determine the intracel-

lular expression of ribozymes quantitatively and qualitatively. Reporter gene firefly luciferase was cloned at *Bam*HI site of vector pcDNA3 Rz giving rise to recombinant vector pcDNA3 Rz-Luc (Fig. 1D). Similarly, reporter gene EGFP was cloned at *Bam*HI and *Not*I sites of vector pcDNA3 Rz to give rise to recombinant vector pcDNA3 Rz-EGFP (Fig. 1E). Both the ribozyme-fused reporter gene constructs were confirmed by restriction digestion and sequencing.

Construction of HEV 3′ end target vectors

Two kinds of HEV substrate constructs were used for in vitro cleavage reaction: plasmid pUC18 HEV nt 7084–7194 (Fig. 2A, I), which was recently reported by us (Agrawal et al., 2001) as RdRp-binding region, and plasmid pGEM-T Easy nt 6616–7194 (Fig. 2A, II). DNA encoding the 3′ end of HEV was amplified by their specific terminal primers using HEV cDNA nt 6046–7194 pPCR-Script clone reported by us (Panda et al., 1995).

Construction of HEV–luciferase reporter gene expression vector

Infectious HEV cDNA clone pSGI-HEV [I] (AF076239) reported by us (Panda et al., 2000) was digested by *Sac*I and *Xho*I to release HEV 3′ end, 7086–7194 nt, and cloned into the equivalent restriction sites of pSGI (construct: pSGI-HEV 3′ end). Firefly luciferase reporter gene was cloned into the pSGI-HEV 3′ end at the *Bam*HI site (construct: pSGI-HEV 3′ end-Luc) (Fig. 2B, I). As a control, plasmid pSGI-Luc that lacks the HEV 3′ end was constructed (Fig. 2B, II). In both the constructs, expression of the genes was driven by SV40 early promoter and also by T7 promoter.

In vitro transcription and in vitro cleavage reaction

Ribozyme expression plasmids pcDNA3 Rz 7125 and pcDNA3 Rz 7112/7125 were linearized with *Bam*HI and transcribed in vitro by T7 RNA polymerase. The substrate HEV 3′ end RNA plasmids pUC18-HEV 7084–7194 were linearized with *Xho*I and transcribed by T7 RNA polymerase in the presence of α-[^{33}P]UTP and RNA products were treated with RQI DNAse according to the supplier's recommendations (Promega, USA). For in vitro cleavage reaction, equimolar concentrations (0.27 pmol each) of the α-[^{33}P]UTP-labeled substrate RNA and unlabeled ribozymes were preincubated at 90°C for 2 min and then mixed under standard cleavage conditions (50 mM Tris–HCl, pH 7.5, 10 mM $MgCl_2$) in 10 μl of reaction volume and incubated at 37°C for 2 h. The reactions were terminated by adding formamide-loading buffer with EDTA. The products of the cleavage reactions were resolved by electrophoresis on an 8% polyacrylamide/7 M urea gel. The cleaved RNA bands were detected by autoradiography of the dried gels. The cleaved RNA fragments were quantified with the help of a Bio-Rad GS-525 molecular imager (Bio-Rad Laboratories, USA).

Cell culture and transfection

Human hepatoma cell line (HepG2), was maintained in Dulbecco's modified Eagle's medium (Life Technologies, USA) supplemented with 10% heat-inactivated fetal bovine serum (Life Technologies, USA), 10 μg/ml streptomycin, and 100 U/ml penicillin (Sigma, USA). For transfection, exponentially growing HepG2 cells were seeded onto 30-mm tissue culture petriplates at a density of 2×10^5 cells per plate and incubated overnight (at least 18 h) to yield 50–70% confluency on the day of transfection. Cationic-lipid-mediated (Lipofectamine Plus Reagent, Life Technologies, USA) transfection was carried out in accordance with the manufacturer's guidelines with a combination of 1 μg of target plasmids (pSGI-HEV 3′ end-Luc/pSGI-HEV [I]) and 1–3 μg of ribozyme plasmids (pcDNA3 Rz 7125 and pcDNA3 Rz 7112/7125). 0.5 μg of plasmid pRL-SV40 (Promega, USA) containing Renilla luciferase gene (R-Luc) was cotransfected as an internal control. Luciferase activity was determined 48 h after cotransfection with a Dual-Luciferase Reporter Assay (Promega, USA) according to the manufacturer's instructions. R-Luc activity was detected to normalize the variation of transfection efficiency among different samples. All the experiments were repeated at least thrice and results reported were reproducible and expressed as the mean $\pm$ SD in relative light units RLU/mg protein or as percentage of activity. Light emission was measured by TD 20/20 Luminometer (Promega, USA).

Total RNA extraction and slot-blot analysis

Two days after transfection, cells were harvested and lyzed in Trizol solution (Life Technologies, USA), and total RNA was isolated by chloroform extraction and isopropanol precipitation. The slot-blot analysis was carried out by standard method (Maniatis et al., 1989). Thirty micrograms of total RNA was immobilized onto a Hybond-N^+ nylon membrane (Amersham Pharmacia Biotech, UK) by gentle suction with a blotting manifold (Life Technologies, USA). Hybridization was carried out by adding α-[^{33}P]UTP (BRIT, INDIA) labeled in vitro transcribed antisense ribozyme RNA (Di-Rz and Mono-Rz) and incubating the membrane at 42°C overnight. The relative ribozyme expression levels were determined by using radiodensitometry.

RT–PCR detection of HEV 3′ end RNA

Equal amounts of RNA (1 μg) were taken and subjected to RT–PCR using the cyclic conditions and HEV 3′ end-specific terminal primers as described earlier (Agrawal et al., 2001). The control RNA (587 bp), human glyceraldehyde-3-phosphate dehydrogenase (hGAPDH) was amplified from its specific terminal primers (Weinberg et al., 2000). A

standard curve of HEV 3′ end RNA was made from a 10-fold serial dilution of the in vitro transcribed HEV 3′ end RNA from the linearized plasmid pUC18-HEV 3′ end 7084–7194 was reverse transcribed by gene-specific reverse primer with 100 U of MMLV reverse transcriptase enzyme (Life Technologies, USA) into cDNA, which was then amplified by real-time PCR using SYBR-Green PCR mix (ABI, USA) with the specific primers of HEV 3′ end (Yang et al., 2002). The Perkin–Elmer ABI Prism 7700 Sequence Detection System was used for real-time analysis.

Acknowledgments

This study was funded by grant-in-aid project from the Department of Science and Technology, Government of India to Professor S.K. Panda. Bandi Sriram and Deepshi Thakral are Research Fellows of Council of Scientific and Industrial Research at the Department of Pathology, All India Institute of Medical Sciences, New Delhi, India.

References

Agrawal, S., Gupta, D., Panda, S.K., 2001. The 3′ end of Hepatitis E virus (HEV) genome binds specifically to the viral RNA dependent RNA polymerase (RdRp). Virology 282, 87–101 doi:10.1006/viro.2000.0819.

Bradely, D.W., 1990. Enterically transmitted non-A, non-B hepatitis. Br. Med. Bull. 46, 442–461.

Bramlage, B., Alefelder, S., Marsehall, P., Eckstein, F., 1999. Inhibition of luciferase expression by synthetic hammerhead ribozymes and their cellular uptake. Nucleic Acids Res. 27, 3159–3167.

Chen, C.J., Banerjea, A.C., Harmison, G.G., Haglund, D., Schubort, M., 1992. Multitarget-ribozyme directed to cleave at up to nine highly conserved HIV-1 *env* RNA regions inhibits HIV-1 replication potential effectiveness against most presently sequenced HIV-1 isolates. Nucleic Acids Res. 20, 4581–4589.

Dahm, S.C., Uhlenbeck, O.C., 1991. Role of divalent metal ions in the hammerhead RNA cleavage reaction. Biochemistry 30, 9464–9469.

Feng, Y., Kong, Y.U., Wang, Y., Qi, G.R., 2001. Intracellular inhibition of the replication of hepatitis B virus by hammerhead ribozymes. J. Gastroenterol. Hepatol. 16, 1125–1130.

James, W., Shamhkani, A., 1995. RNA enzymes as tools for gene ablation. Curr. Opin. Biotechol. 6, 44–49.

Kabrane-Lazizi, Y., Meng, X.J., Purcell, R.H., Emerson, S.U., 1999. Evidence that the genomic RNA of hepatitis E virus is capped. J. Virol. 73, 8848–8850.

Macejak, D.G., Jensen, K.L., Jamison, S.F., Domenico, K., Roberts, E.C., Chaudhary, N., Carlowitz, I.V., Bellon, L., Tong, M.J., Conrad, A., Pavco, A.P., Blatt, M.L., 2000. Inhibition of Hepatitis C virus (HCV) RNA dependent translation and replication of a chimeric HCV Poliovirus using synthetic stabilized ribozymes. Hepatology 31, 769–776.

Maniatis, T., Fritsch, E.F., Sambrook, J., 1989. Molecular Cloning: A Laboratory Manual. Cold Spring Harbor Laboratory Press, Cold Spring Harbor, NY.

Panda, S.K., Jameel, S., 1997. Hepatitis E virus: from epidemiology to molecular biology. Viral Hepatitis Rev. 3, 227–251.

Panda, S.K., Ansari, I.H., Durgapal, H., Agrawal, S., Jameel, S., 2000. The in vitro synthesized RNA from a cDNA clone of Hepatitis E virus is infectious. J. Virol. 74, 24330–24337.

Panda, S.K., Nanda, S.K., Zafrullah, M., Ansari, I.H., Ognener, M.H., Jameel, S., 1995. An Indian strain of hepatitis E virus (HEV): cloning, sequencing and expression of structural region and antibody responses in sera from individuals from an area of high-level HEV endemicity. J. Clin. Microbiol. 33, 2653–2659.

Parthasarathy, R., Cote, G.J., Gagel, R.F., 1999. Hammerhead ribozyme mediated inactivation of mutant RET in medullary thyroid carcinoma. Cancer Res. 59, 3911–3914.

Purcell, R.H., Ticehurst, J.R., Enterically transmitted non-A, non-B hepatitis: epidemiology and clinical characteristics, in: Viral Hepatitis and Liver Diseases, New York, 1988, pp. 133–137.

Purdy, M.A., Tam, A.W., Huang, C.C., Yarbough, P.O., Reyes, G.R., 1993. Hepatitis E virus: a non-enveloped member of the alpha-like RNA virus super group. Semin. Virol. 4, 319–326.

Sakamoto, N., Wu, H.C., Wu, Y.G., 1996. Intracellular cleavage of Hepatitis C virus RNA and inhibition of viral protein translation by hammerhead ribozymes. J. Clin. Invest. 98, 2720–2728.

Santoro, S.W., Joyce, 1997. A general purpose RNA-cleaving DNA enzyme. Proc. Natl. Acad. Sci. USA 94, 4262–4266.

Song, C., Simon, A.E., 1995. Requirement of a 3′ terminal stem loop in in vitro transcription by an RNA dependent RNA polymerase. J. Mol. Biol. 254, 6–14.

Tyagi, S., Korkaya, H., Zafrullah, M., Jameel, S., Lal, S.K., 2002. The phosphorylated form of the ORF3 protein of hepatitis E virus interacts with its non-glycosylated form of the major capsid protein, ORF2. J. Biol. Chem. 277, 22759–22767.

Uhlenbeck, O.C., 1987. A small catalytic oligoribonucleotide. Nature 328, 596–600.

Weinberg, M., Passman, M., Kew, M., Arbuthnot, P., 2000. Hammerhead ribozyme mediated inhibition of hepatitis B virus X gene expressed in cultured cells. J. Hepatol. 33, 142–151.

Yang, J.H., Lai, J.P., Douglas, S.D., Metger, D., Zhu, X.H., Ho, W.Z., 2002. Real-time RT-PCR for quantitation of hepatitis C virus RNA. J. Virol. Methods 102, 119–128.